Int. J. Electrochem. Sci., 12 **(2017)** 4456 – 4464, doi: 10.20964/2017.05.19

International Journal of
ELECTROCHEMICAL
SCIENCE
www.electrochemsci.org

Double-layer Si/TiO_2NTAs as High Performance Anode for Li-ion Batteries

Binlin Guo, Jing Wu, Yong Zhang, Shanshan Li, Yue Zhang, and Yadong Wang[*]*, and Mu Pan*

State Key Laboratory of Advanced Technology for Materials Synthesis and Processing, Wuhan University of Technology, Wuhan430070, P. R. China
[*]E-mail: ywang@whut.edu.cn

Received: 13 January 2017 / *Accepted:* 6 March 2017 / *Published:* 12 April 2017

In this paper, a novel three-dimensional TiO_2 nanotube arrays (TiO_2NTAs) structure was introduced into a silicon electrode. The TiO_2NTAs acted as both electrochemically active materials and buffers to maintain structural integrity. An initial capacity of 5320 mAh/g was realized, and a The capacity of 1500 mAh/g was maintained after 120 charge/discharge cycles. This good capacity retention benefits from the establishment and maintenance of the excellent structural integrity granted by the introduction of the special TiO_2NTAs.The superior ability of the TiO_2NTAs for stress buffering and space accommodation allows the silicon electrode to maintain lower charge transfer resistance during long cycling.

Keywords: lithium-ion batteries; anode material; silicon; TiO_2 nanotube arrays; cycling stability

1. INTRODUCTION

Silicon (Si) is considered to be one of the most promising anode materials for the next generation of lithium-ion batteries (LIBs) due to its large theoretical electrochemical capacity of 3578 mAh/g in the form of $Li_{15}Si_4$[1]. The low cost, high abundance, and environmental friendliness of silicon electrode materials offer large advantages for commercial applications[2]. However, Si-based anode materials are subject to dramatic volume changes during lithiation/delithiation, leading to the destruction of the solid electrolyte interface (SEI) and the degradation of their mechanical integrity, which has seriously affected the cycling performance of Si-based anode materials[3-4].

To improve the cycling performance and coulombic efficiency of Si-based anode materials, many efforts have been devoted to the nanoparticulation of active materials[5-6], surface modification[7], new morphology and structure design[8], binder development[9], and novel

electrolyte and additive investigation[10]. Although the electrochemical performance of silicon-based electrodes has seen effective improvement through the above-mentioned efforts [11-12], tedious, energy-intensive experimental procedures and the use of high-cost materials greatly limit their practical applications. Considering this issue, it is necessary to explore facile, low-cost and effective methods to obtain excellent electrochemical performance to facilitate the real commercial application.

Mechanical and structural electrode integrity play a critical role during the charging/discharging of Li-ion batteries, which directly affects their coulombic efficiency and cycling stability. A few studies have shown that the capacity loss could be fully regained when an external force was used to reconnect the electrical contact[13]. Therefore, maintaining the electrode integrity of a Si-based anode is a key issue when designing an electrode structure. Herein, inspired by the double-layered electrode design [14], we report a novel Si/TiO_2NTAs(TiO_2 nanotube arrays) electrode structure that places a TiO_2NTAs layer between the active silicon electrode layer and the titanium current collector. The TiO_2NTAs film was directly grown on the titanium substrate. Figure 1 schematically illustrates the electrode structure and its action mechanisms. The film of TiO_2NTAs between the active materials and the titanium substrate possesses various characteristics, such as top opening, uniform cell size, and strong adhesion to the substrate. These superior characteristics are favorable for the mechanical and structural integrity of the silicon electrode during charge/discharge cycling. First, the TiO_2NTAs layer will buffer the large volume change during lithiation/delithiation. Second, the stronger adhesion between silicon active materials compared to a direct coating of silicon on the current collector can depress the peeling-off of the active materials from the substrate. Moreover, the highly ordered tube openings of the TiO_2NTAs provide extra space for the volume expansion of Si, averting the destruction of the electrode. Furthermore, the TiO_2NTAs will also provide capacity as active materials showing a more prominent advantage compared to other non-active buffer materials. This simple but helpful electrode structure design will provide a new solution for electrochemical performance improvement of silicon-based electrode.

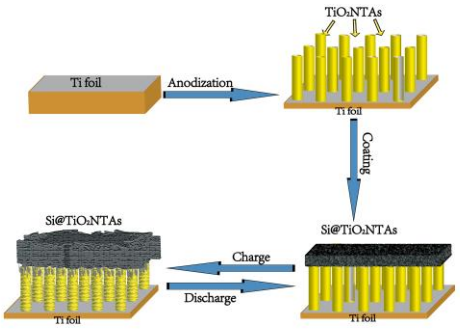

Figure 1. Schematic structural illustrations of the double-layer Si/TiO_2NTAs electrode

2. EXPERIMENTAL

2.1 Synthesis of TiO2NTAs

The TiO_2 nanotube arrays were prepared by using an anodic oxidation method. Prior to anodization, industrial pure titanium foils (0.1 mm thick, 99.7% purity) were cut into 8 mm×8 mm

pieces and treated sequentially by sonication in acetone for 30 min, rinsing with DI water and drying in ambient conditions. The anodization process was conducted using a two-electrode system at room temperature. Ti foil acted as the working electrode, and a Cu sheet served as the counter electrode. The electrolyte was NH_4F (0.4 wt%) in a mixture of ethylene glycol and DI water (8:1 in volume). The anodization was carried out with a DC power source under a constant voltage of 60V for 2 h. After anodization, the Ti foils were rinsed repeatedly with DI water and then dried in hot air. Finally, the samples were annealed in air at 500 ℃for 1 h using a heating rate of 5 ℃/min for crystallization.

2.2 Electrode fabrication and electrochemical measurements

For the fabrication of the electrodes, a bulk Si (200 mesh) slurry (Si: Super p: PVDF=2:6:2)was prepared. The active material electrode was fabricated by coating the Si slurry onto the prepared TiO_2NTAs and vacuum drying in an oven at 80 ℃for 12 h. All the electrochemical measurements were carried out using 2025 coin cells. The cell was assembled in a glove box filled with argon to maintain the level of H_2O and O_2 below 0.1 ppm. The Si/TiO_2NTAs electrode served as the working electrode while the pure lithium foils were used as the counter electrode. The electrolyte was 1 M $LiPF_6$ in EC: DEC (1:1 by volume). The electrochemical performance of all the cells was tested between 0.01–3.0 V using a LAND-CT2001A battery test system unless specified otherwise. Electrochemical impedance spectroscopy (EIS) analysis was performed on an electrochemical workstation (CHI-604D) within the frequency range of 0.01-100kHz. Cyclic voltammetry was performed between the voltage range of 0.01– 3.0 V with a scan rate of 0.1 mV/s.

2.3 Materials characterization

Scanning electron microscopy (SEM) (Zeiss Ultra Plus) was performed to observe the morphology change of the active material before and after cycling. X-ray diffraction (XRD) measurements were performed on a diffractometer (D/MAX-RB RU-200B) with Cu Kα radiation (λ=1.54145 Å) generated at 40kV and 50 mA. Scans for 2θ values were recorded at 10° min^{-1} (20°~80°).

3. RESULTS AND DISCUSSION

Figure.2 shows the X-ray pattern of the double-layer Si/TiO_2NTAs electrode. A traditional single-layer Si electrode was also measured as a comparison. The TiO_2 arrays show clear diffraction peaks attributed to anatase crystallization. Diffraction peaks for crystallized silicon can also be observed.

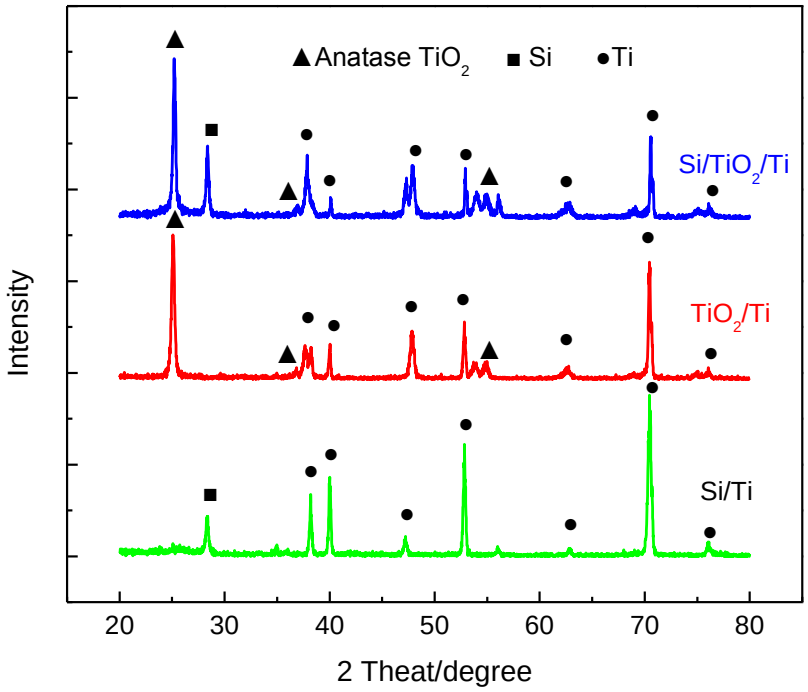

Figure 2. XRD patterns of TiO_2/Ti films, Si/TiO_2NTAs films, and Si/Ti films.

The electrochemical activity of Si/TiO_2NTAs as a lithium-ion anode was first examined by cyclic voltammetry (CV). A silicon electrode coated on the same titanium substrate (denoted as a single-layer silicon electrode) was also tested as a comparison. The experimental results are shown in Figure 3. The shapes of the CV curves for the two electrodes in the lower potential range below 1.0 V are similar. Both CV curves show the SEI film formation band at 0.75 V in the first lithiation cycle[15]. The lower potential region (0.01-0.75 V), a cathodic peak at approximately 0.2 V, which appears in the 2nd cycle and evolves in subsequent cycles, and two extraction peaks located at 0.25 V and 0.5 V, that are attributed to the alloying/de-alloying reaction of Si with Li^+ ions, respectively.[16-17]. However, the area of the lithiation /delithiation peaks for the Si/TiO_2NTAs electrode decreased with cycle number much more slowly than did those of single-layer silicon, suggesting that more stable cycling performance will be obtained for the Si/TiO_2NTAs electrode. In the higher voltage range, the CV curve of the double-layer Si/TiO_2NTAs electrode shows one pair of redox peaks at 1.7V and 2.05V, which can be attributed to the lithiation/delithiation of crystalline TiO_2,respectively[18].

Figure 4a displays the charge−discharge curves of the Si/TiO_2NTAs at a constant current density of 500 mA/g. Three apparent voltage plateaus can be observed in the first discharge curve, which are attributed to the lithium intercalation of the TiO_2NTAs to form an Li_xTiO_2 alloy phase, SEI formation[19], and silicon lithiation, respectively. These features are in good agreement with the CV results. The initial discharge delivers a capacity of 5320 mAh/g. The irreversible capacity loss of the Si/TiO_2NTAs electrode is mainly due to irreversible side reactions of silicon particles during the formation of the SEI, irreversible decomposition of the electrolyte and lithium adsorption in the

conductive carbon black[20]. After 5 cycles, the discharge capacity is 2580 mAh/g, and the capacity tends to be stable thereafter. In contrast, in Figure 4b, the single-layer Si electrode shows a sharp capacity decay, and the capacity was attenuated to 270 mAh/g after 10 charge/discharge cycles.

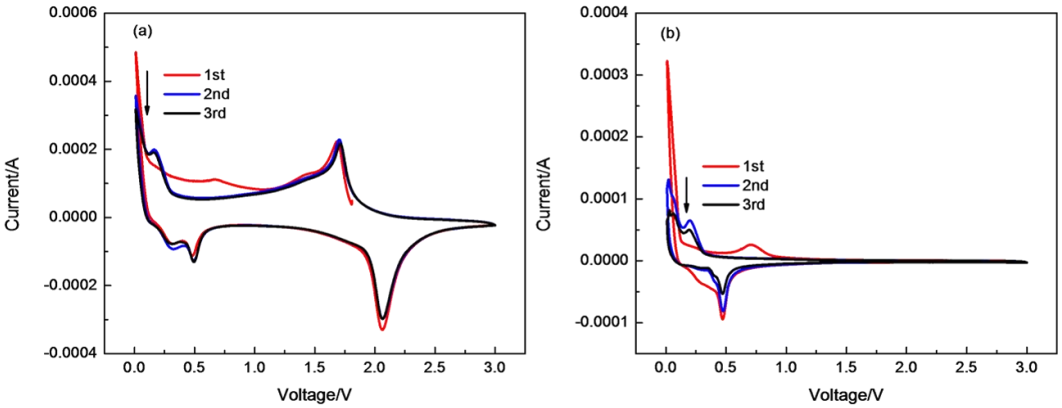

Figure 3. Cyclic voltammetry of the Si/TiO_2NTAs electrode (a) and the single-layer Si electrode (b).

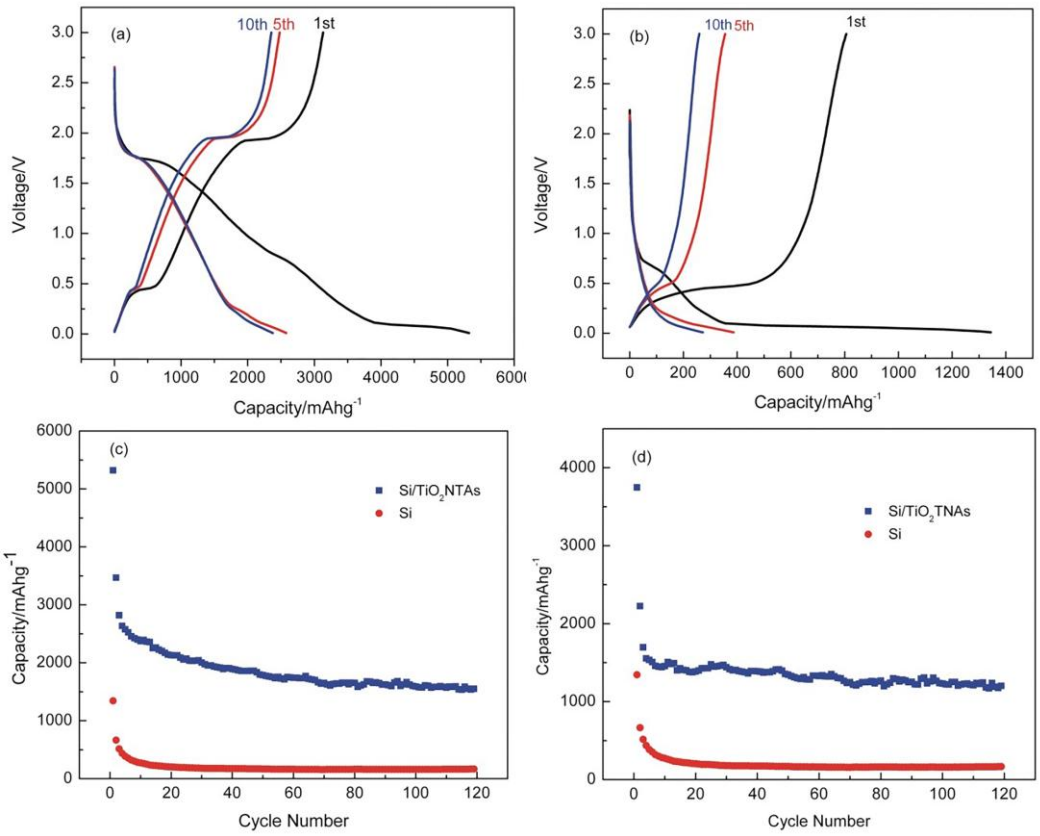

Figure 4. The cycling performance comparison of Si/TiO_2NTAs and Si electrodes. (a) Charge/discharge profile of the Si/TiO_2NTAs electrode, (b) charge/discharge profile of the single-layer Si electrode, (c) galvanostatic cycling profiles, (d) gavanostatic cycling profile with TiO_2 capacity subtraction.

To evaluate the cycling stability of the Si/TiO_2NTAs electrode, continuous galvanostatic discharge-charge tests were conducted at a current density of 500 mA/g as shown in Figure 4c. A similar test was also carried out for the single-layer Si electrode as a comparison. A capacity of 1550 mAh/g for the Si/TiO_2NTAs electrode was retained after 120 cycles with a coulombic efficiency above 98%. However, a capacity of only 110 mAh/g was obtained for single-layer silicon electrode.

Considering the support film of TiO_2 being involved in the lithiation/delithiation reaction to deliver electrochemical capacity, the lithiation capacity of the TiO_2NTAs should be subtracted to elucidate the direct effect of the special TiO_2NTAs structure to the cycling stability of the silicon electrode. In this modified calculation, the capacity of a TiO_2NTAs electrode obtained in the same charge/discharge protocol was subtracted from the capacity of the Si/TiO_2NTAs electrode. The calculation results are shown in Figure 4d. After 120 cycles, the capacity of the Si/TiO_2NTAs electrode arising from silicon is 1200 mAh/g, which is still more than three and a half times higher than the theoretical capacity of graphite . In addition, careful observation of the cycling profile reveals that the electrode experiences quick capacity decay in only the initial 10 cycles. Afterwards, the capacity remains almost stable. These results indicate that the introduction of the TiO_2NTAs layer can effectively improve the cycling stability. The significant performance improvement of the Si/TiO_2NTAs electrode may be attributed to the stress/strain buffer and space accommodation of the TiO_2NTAs support structure, which not only relieves the volume expansion stress of the Si particles in the lithiation/delithiation reaction but also gradually accommodates the active materials into the TiO_2 hollow nanotubes and the gaps between nanotubes during cycling. As a result, the TiO_2NTAs based support structure restrains the cracking and pulverization of Si particles to some extent, and supplies a relative stable reaction space and stress for active materials during charge/discharge cycling. Compared to other related works, our investigation has a simplified preparation process, and the as-synthesized electrode shows significant improvements of capacity and cycling performance.

To further resolve the possible effect of the TiO_2NTAs support on the silicon electrode, FESEM images of the Si/TiO_2NTAs and Si electrodes were recorded to observe the cross-sectional morphology change before and after galvanostatic charge/discharge (Figure. 5a-d). The single-layer Si electrode shows some obvious gaps between the Si, conductive additive, binder film and the substrate, which suggests relatively unstable adhesion between the active materials and the current collector. After 50 charge/discharge cycles, most of the active materials of the single-layer Si electrode exfoliate from the substrate, and resulting in pulverization. Pulverization is one of the critical reasons for the low cycling performance of silicon electrodes. In contrast, the Si/TiO_2NTAs layer adheres strongly to the substrate through the TiO_2NTAs, which directly grow on the current collector. The special dense hollow structure of the TiO_2NTAs may also enhance the bonding power between the active materials and TiO_2NTAs film. It can be clearly seen from the cross-section of the Si/TiO_2NTAs electrode after 50 cycles that the volume expansion was restrained effectively and very little of the active material had fallen off the TiO_2NTAs film. It is worth noting that the TiO_2NTAs remained well-aligned before and after the cycling, indicating the effective buffer effect of the TiO_2NTAs to the mitigation of the stress due to the volume change of the silicon particles. The TiO_2NTAs appeared to be more viscous after 50 cycles, and the hollow space was gradually filled, which was considered evidence that the Si particles had extended into the hollow space during volume expansion, thereby relieving the damage to the

integral structure of the Si/TiO_2NTAs electrode, and granting significantly improves cycling performance.

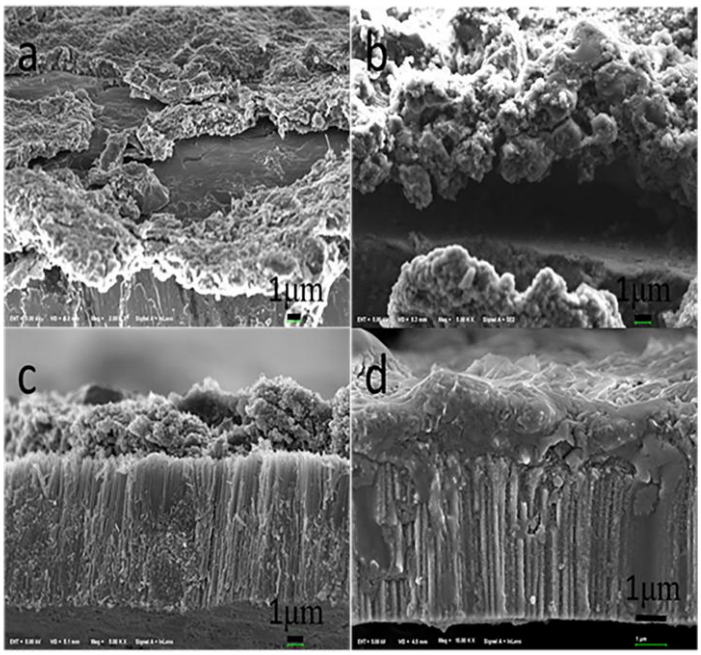

Figure 5. FESEM images of the Si electrode before (a) and after 50 cycles(b), and the Si/TiO_2NTAs electrode before(c) and after 50 cycles(d).

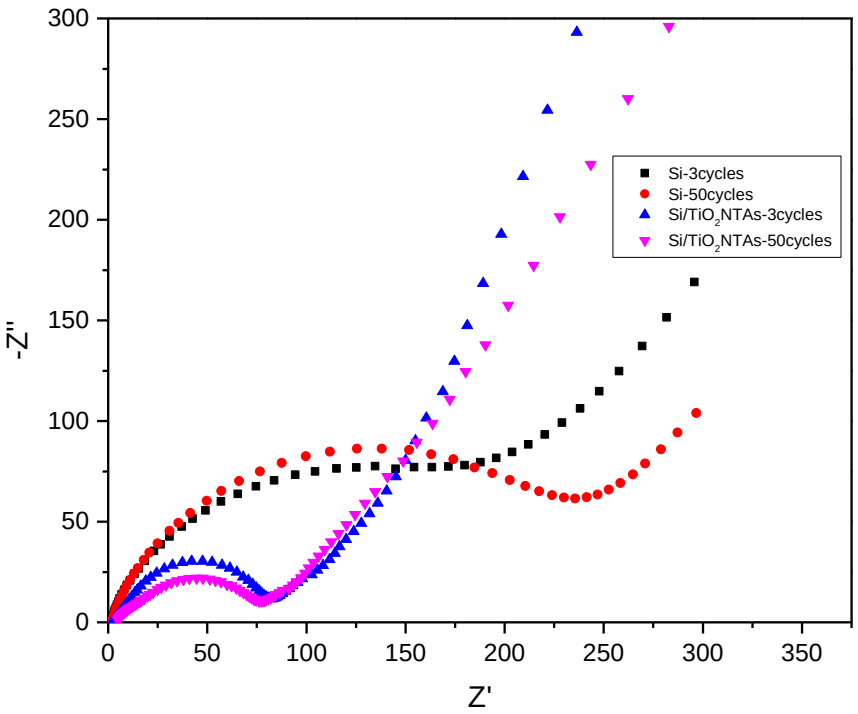

Figure 6. EIS spectra of Si/TiO_2NTAsand single-layer silicon electrodes on the 3rd and 50th cycles before (a) and after discharge to 500 mV.

EIS measurements were also conducted to further investigate the interface reactions between the electrolyte solution and the electrode as shown in Figure 6. The depressed semicircle in the high and middle frequency is associated with lithium ion migration through the SEI film, and the charge transfer reaction. The inclined line at lower frequencies is attributed to the Warburg impedance, which represents the lithium ion diffusion process within the electrodes [21]. The diameter of the semicircle for the Si/TiO_2NTAs electrode is much smaller than that for the single-layer silicon electrode, suggesting lower charge transfer resistance for the Si/TiO_2NTAs electrode. After 50 cycles, the charge transfer resistance of the Si/TiO_2NTAs electrode showed no obvious change. However, a large increase of the charge transfer resistance was observed for the single-layer silicon electrode. These EIS results indicate that the introduction of the TiO_2NTAs not only contributed to the fast charge transfer of the initial cycles but also helped maintain the low resistance during long cycles. The lower charge transfer resistance should be attributed to the establishment and maintenance of excellent structural integrity of the Si/TiO_2NTAsbecause of the implantation of TiO_2NTAs, just as shown in SEM results.

4. CONCLUSION

A novel double-layer Si/TiO_2NTAs electrode structure was constructed to improve the cycling stability of the silicon electrode. TiO_2 is electrochemically active for rechargeable lithiation. TiO_2NTAs contribute not only to the capacity improvement but also to the excellent cycling performance. A high initial capacity of 5320 mAh/g was realized. This capacity of 1500 mAh/g was retained after 120 charge/discharge cycles. This good capacity retention was attributed to the establishment and maintenance of the excellent structural integrity granted by the stress buffering and space accommodation of the TiO_2NTAs. The introduction of TiO_2NTAs can be used as a feasible and effective method to broaden the commercial applications of silicon-based anodes.

ACKNOWLEDGEMENTS
This research was supported by the National Science Foundation of China (21473128 and 21373154).

References

1. T.D. Hatchard, J.R. Dahn, *J. Electrochem. Soc*, 151 (2004) A838.
2. J.R. Szczech, S. Jin, *Energ Environ Sci*, 4 (2011) 56.
3. Y. Chen, S. Zeng, J. Qian, Y. Wang, Y. Cao, H. Yang, X. Ai, *ACS Appl. Mat. Interfaces*, 6 (2014) 3508.
4. H. Wu, G. Chan, J.W. Choi, I. Ryu, Y. Yao, M.T. Mcdowell, S.W. Lee, A. Jackson, Y. Yang, L. Hu, *Nature Nanotech*, 7 (2012) 310.
5. U. Kasavajjula, C. Wang, A.J. Appleby, *J. Power Sources*, 163 (2007) 1003.
6. Z.P. Guo, J.Z. Wang, H.K. Liu, S.X. Dou, *J. Power Sources*, 146 (2005) 448.
7. W. Xu, S.S.S. Vegunta, J.C. Flake, *J. Power Sources*, 196 (2011) 8583.
8. L.F. Cui, Y. Yang, C.M. Hsu, Y. Cui, *Nano Letters*, 9 (2009) 3370.
9. B. Koo, H. Kim, Y. Cho, K.T. Lee, N.S. Choi, J. Cho, *Angew. Chem. Int. Ed*, 51 (2012) 8762.
10. I.A. Profatilova, C. Stock, A. Schmitz, S. Passerini, M. Winter, *J. Power Sources*, 222 (2013) 140.

11. T. Song, L. Hu, U. Paik, *J.phys.chem.lett*, 5 (2014) 720.
12. T.M. Higgins, S.H. Park, P.J. King, C.J. Zhang, N. Mcevoy, N.C. Berner, D. Daly, A. Shmeliov, U. Khan, G. Duesberg, *Acs Nano*, (2016).
13. C.K. Chan, H. Peng, G. Liu, K. Mcilwrath, X.F. Zhang, R.A. Huggins, Y.I. Cui, *Nature Nanotech*, 3 (2008) 31.
14. Z. Yang, Y. Xia, J. Ji, B. Qiu, K. Zhang, Z. Liu, *RSC Adv* 6(2016) 12107.
15. H. Ota, Y. Sakata, A. Inoue, S. Yamaguchi, *J. Electrochem. Soc*, 151 (2004) A1659.
16. M.N. Obrovac, L.J. Krause, *J. Electrochem. Soc*, 154 (2007) A103.
17. S. Zhang, T. Jiang, R. Lin, G. Liu, W. Liu, *Int J electrochem sc*, 8 (2013) 9644.
18. D. Bresser, E. Paillard, E. Binetti, S. Krueger, M. Striccoli, M. Winter, S. Passerini, *J. Power Sources*, 206 (2012) 301.
19. B.D. Polat, O. Keles, K. Amine, *Nano Letters*, 15 (2015).
20. Y. Bai, D. Yan, C. Yu, L. Cao, C. Wang, J. Zhang, H. Zhu, Y.S. Hu, S. Dai, J. Lu, *J. Power Sources*, 308 (2016) 75.
21. S.L. Chou, J.Z. Wang, M. Choucair, H.K. Liu, J.A. Stride, S.X. Dou, *Electrochem. Commun*, 12 (2010) 303.